Ceramics International 42 (2016) 11363–11372

Contents lists available at ScienceDirect

Ceramics International

journal homepage: www.elsevier.com/locate/ceramint

Effect of ZrO_2 content on ageing resistance and osteogenic cell differentiation of ZrO_2–Al_2O_3 composite

María P. Albano [a,*], Heidy L. Calambás Pulgarin [a], Liliana B. Garrido [a], Emanuela Prado Ferraz [b], Adalberto L. Rosa [b], Paulo Tambasco de Oliveira [b]

[a] Centro de Tecnología de Recursos Minerales y Cerámica (CETMIC), CCT-La Plata CONICET, CICPBA, C.C. 49 (B1897ZCA), M. B. Gonnet, Provincia de Buenos Aires, Argentina

[b] School of Dentistry of Ribeirão Preto, University of São Paulo (FORP-USP), Av. Do Café, s/n-Campus USP Monte Alegre, 14040-904 Ribeirão Preto, São Paulo, Brazil

ARTICLE INFO

Article history:
Received 11 March 2016
Received in revised form
12 April 2016
Accepted 13 April 2016
Available online 14 April 2016

Keywords:
Al_2O_3–ZrO_2
Ageing behavior
Phase transformation
Osteoblast cell cultures
Mineralization

ABSTRACT

Two commercial 3 mol% yttria-partially stabilized zirconia powders, with 0.3 wt% Al_2O_3 (YZA) and without Al_2O_3 (YZ), were used to produce alumina (Al_2O_3)–zirconia (ZrO_2) slip cast composites. The influence of the ZrO_2 content and the ZrO_2 grain size on the ageing behavior of the different Al_2O_3–ZrO_2 composites was investigated. In addition, the *in vitro* biocompatibility and osteogenic cell differentiation of Al_2O_3–ZrO_2 surfaces were evaluated before ageing (ba) and after ageing (aa) using the rat bone marrow-derived osteoblast cell culture model; the osteogenic potential of preosteoblast MC3T3-E1 cells on the same surfaces was also assessed. The ageing susceptibility of the composites significantly increased with increasing the ZrO_2 content over 22 vol%. For ZrO_2 contents $\leq$ 22 vol%, the grain size did not influence the transformability of tetragonal ZrO_2 under ageing conditions; however, in the composites with 50 vol%, the greater grain size of 50 vol% YZ with respect to 50 vol% YZA enhanced the ageing degradation. Overall, the cell culture experiments revealed no significant differences among the composites before ageing in terms of osteogenic cell differentiation, except for the higher mineralization of bone marrow-derived osteoblast cells grown on 50 vol% YZ ba compared with the ones grown on 50 vol% YZA ba. The ageing process tended to rescue the osteogenic potential of these cells grown on 50 vol% YZA while inhibiting the one on 50 vol% YZ. In conclusion, the low ageing sensitive of the composites with ZrO_2 contents $\leq$ 22 vol% did not change the osteoblast biocompatibility, whereas the greater ageing degradation of the composites with 50 vol% ZrO_2 seemed to alter the osteogenic potential of bone marrow-derived osteoblast cells.

1. Introduction

Zirconia-toughened-alumina (ZTA) ceramics are currently of great interest for biomedical applications, as an alternative to biomedical-grade alumina and zirconia [1,2]. Indeed, alumina has moderate fracture toughness, and serious problems have been reported with yttria-stabilized zirconia (Y-TZP) ageing degradation used in total hip replacement [3]. The problem with Y-TZP was caused by the low temperature degradation (LTD) of zirconia, the so-called ageing process. When Y-TZP is exposed to an aqueous environment at 100–300 °C over long periods, the surface of the Y-TZP transforms spontaneously into the monoclinic structure via a stress-corrosion-type mechanism [4]. This transformation is accompanied by a 4 vol% increase and 16% shear, leading to microcracking, surface roughening, and eventually grain pullout. The process continuously proceeds from the surface to the bulk of Y-TZP, resulting in a volumetric expansion followed by failure [4]. Using ZTA, improved mechanical properties such as strength and crack propagation resistance could be obtained [5]. However, since these ceramics contain zirconia, they are likely to undergo ageing.

In this work, two commercial 3 mol% yttria-partially stabilized zirconia powders, with 0.3 wt% Al_2O_3 (YZA) and without Al_2O_3 (YZ), were used to produce Al_2O_3-ZrO_2 slip cast composites with different zirconia contents. In a recent paper [2], we have studied the influence of the zirconia content on the sintering behavior and microstructure development of Al_2O_3–ZrO_2 composites. The microstructural characterization revealed that the composites obtained by using YZ and YZA had different zirconia mean grain sizes [2]. The ageing susceptibility of Y-TZP is strongly dependent on its grain size [6].

It is believed that the zirconia content and the different physicochemical characteristics of YZ and YZA powders may affect the

* Corresponding author.
E-mail address: palbano@cetmic.unlp.edu.ar (M.P. Albano).

http://dx.doi.org/10.1016/j.ceramint.2016.04.063
0272-8842/

Al_2O_3–ZrO_2 biocompatibility. In addition, the zirconia tetragonal (t)-monoclinic (m) transformation during ageing can induce cell proliferation due to the creation of a roughness surface layer of monoclinic phase on the Al_2O_3–ZrO_2 ceramics. In this work, the influence of the ZrO_2 content and the ZrO_2 grain size on the ageing behavior of Al_2O_3-YZ and Al_2O_3-YZ was investigated. In addition, the biocompatibility and osteogenic cell differentiation of the different Al_2O_3-ZrO_2 surfaces were evaluated before and after ageing using osteoblast cell cultures.

2. Experimental procedure

2.1. Ceramic preparation and characterization

3 mol% yttria-partially stabilized zirconia with 0.25 wt% Al_2O_3 (YZA) (Saint-Gobain ZirPro, China) and without Al_2O_3 (YZ) (Saint-Gobain ZirPro, China) powders were used in this study. The composition and physical properties of the two zirconia powders are shown in Table 1. The mean particle size of YZA and YZ was 0.21 μm and 0.40 μm, respectively. Al_2O_3–ZrO_2 compositions with different YZA and YZ contents, 10.5, 22 and 50 vol%, were used to prepare the composites.

A commercial ammonium polyacrylate solution (NH_4PA) (Duramax D 3500, Rohm & Haas, Philadelphia, PA) was used as deflocculant. 48 vol% aqueous Al_2O_3-ZrO_2 suspensions with the different compositions and the optimum NH_4PA concentration were prepared by suspending particles in deionized water via 40 min of ultrasound; the pH was manually adjusted to be maintained at 9 with ammonia (25%). Slips were cast in plaster molds into rectangular bars (12 × 10 × 9 mm); the consolidated bars were dried slowly in air for 24 h at room temperature (RT) and 24 h at 100 °C. The green samples were sintered in air at 1600 °C for 2 h (heating rate 5 °C/min).

The zirconia grain sizes were measured using SEM micrographs (JEOL, JSM-6360) of polished and thermally etched surfaces. The grain size values were the average of about a hundred measurements.

The biological assays were carried out using Al_2O_3–ZrO_2 disks, 12 mm in diameter and 3 mm thickness, produced by slip casting and sintered at 1600 °C for 2 h.

2.2. Al_2O_3–ZrO_2 ageing

The ageing degradation experiments were carried out in an autoclave at a temperature of 134 °C under 2-bars pressure at increasing time up to 24 h (1 h in autoclave is theoretically equivalent to 3–4 years *in vivo* [7]). This treatment is therefore a good indicator of the ageing sensitivity *in vivo* of a given alumina-zirconia ceramic.

Phase identification was done by X-ray diffraction (XRD) analysis (Philips 3020 equipment) using Cu-Kα radiation with Ni filter at 40 kV–20 mA. The influence of the ageing on the zirconia t-m transformation was quantitatively evaluated by XRD. The volume fractions of monoclinic and tetragonal ZrO_2 on the surfaces of the composites were calculated using the Rietveld method [8]. Sintered samples before and after ageing were cut and polished for microstructural observation by SEM on the cross section of the samples. The changes in surface topography after ageing were examined by AFM (Multimode-Nanoscope V, Veeco, Santa Barbara, CA) in contact mode. The used silicon nitride probes had a nominal spring constant of 0.06 N/m and a nominal tip radius of curvature of 10 nm.

Table 1
Composition and physical properties of the different ZrO_2 powders.

Composition and properties	YZ	YZA
Y_2O_3 (wt %)	5.29	5.32
Al_2O_3	50 ppm	0.25 wt%
d_{50} (μm)	0.40	0.21
Sg (m^2/g)	7.8	12.2
IEP	7	8.9
Zeta potential at pH 7.5 (mV)	−10	27

2.3. Biological assays

2.3.1. Cell culture

2.3.1.1. Cell isolation and culture of bone marrow-derived osteoblast cells. The cells were obtained from bone marrow of young adult male rats (Rattus norvegicus, Wistar) weighing 120 g as described previously [9], under the guidance of the Ethics Committee on Animal Use of the University of São Paulo at Ribeirão Preto (Protocol Number 2015.1.1136.58.1). The animals were euthanized by an overdose of chemical anesthetics Ketamin (Agener União, São Paulo, Brazil). Briefly, the femora were excised aseptically, cleaned of soft tissues, and passed through 2 washes of culture medium containing 10 times the usual concentration of antibiotics, composed by standard culture medium consisting of a minimal essential medium (MEM, Invitrogen, Carlsbad, CA), 500 μg/mL gentamycin (Invitrogen) and 3 μg/mL fungizone (Invitrogen). The epiphysis of the bones were removed, and the marrow flushed out using 5 mL of culture medium expelled from a 10 mL syringe through a 20-gauge needle. The released cells were collected in a 75 cm^2 culture flask (Corning Incorporated, NY) containing 10 mL of osteogenic medium (OM) composed by MEM supplemented with 10% fetal bovine serum (Invitrogen) and 500 μg/mL gentamycin (Invitrogen) supplemented with 5 μg/mL ascorbic acid, 7 mM glycerophosphate (Sigma-Aldrich, St. Louis, MO), and 10^{-7} M dexamethasone (Sigma-Aldrich). The flasks were incubated at a 37 °C in a humidified atmosphere of 5% CO_2 and 95% air. The medium was changed every 3 days. After 7–10 days, first passage cells were counted and seeded in 24-well culture plates (Corning) containing the disks immersed in 1.8 mL of OM, at a plating density of 2×10^4 cells/well. Cells seeded in wells without disks were used as controls. During the culture period, cells were incubated at 37 °C in a humidified atmosphere of 5% CO_2 and 95% air, for up to 17 days.

2.3.1.2. Culturing of preosteoblast MC3T3-E1 cells. The preosteoblast MC3T3-E1 cells (subclone 14) were obtained from the American Type Culture Collection (ATCC) and cultured in growth medium (α-MEM - alpha-minimum essential medium, Life Technologies, Grand Island, NY) supplemented with 10% bovine fetal serum (Gibco, Grand Island, NY), 50 μg/mL gentamicin (Gibco) and 0.3 μg/mL fungisone (Gibco) in 75 cm^2 flasks (Corning Inc., Costar, Corning, NY) until subconfluence [10]. Cells were then harvested after treatment with 1 mM ethylenediamine tetraacetic acid (EDTA) (Gibco) and 0.25% trypsin (Gibco). First passage cells were cultured in 24-well culture plates on disks at a cell density of 2×10^4 cells per disc in OM, which was growth medium supplemented with 5 μg/mL ascorbic acid (Gibco) and 7 mM β-glycerophosphate (Sigma-Aldrich, St. Louis, MO) for up to 21 days. Cultures were kept at 37 °C in a humidified atmosphere of 5% CO_2 and 95% air; the medium was changed every 2 days.

2.3.2. Cell morphology

At day 1 of culture, bone marrow-derived osteoblast cell morphology was evaluated by direct fluorescence to detect the actin cytoskeleton and cell nuclei [11]. Briefly, cells were fixed for 10 min at RT using 4% paraformaldehyde in 0.1 M sodium phosphate buffer (PB), pH 7.2. After being washed in PB, cultures were

permeabilized with 0.5% Triton X-100 in PB for 10 min and processed for fluorescence labeling. Alexa fluor 594 (red fluorescence)-conjugated phalloidin (1:200, Molecular Probes, Eugene, OR) was used to label the actin cytoskeleton. Before mounting for microscope observation, samples were washed with deionized water (dH_2O), and the cell nuclei were stained with 300 nM 40,6-diamidino-2-phenylindole, dihydrochloride (DAPI, Molecular Probes) for 5 min. The disks were placed face up on glass slides, covered with 12-mm round glass coverslips (Fisher Scientific, Grand Island, NY) and mounted with an antifade kit (Vectashield, Vector Laboratories, Burlingame, CA). The samples were then examined under epifluorescence, using a Zeiss AxioImager M2 microscope (Carl Zeiss, Oberkochen, Germany) outfitted with an AxioCam MRm digital camera (Carl Zeiss). Acquired digital images were processed with Adobe Photoshop CS5.1 software (Adobe Systems).

2.3.3. Cell viability

Cell viability was evaluated by 3-[4,5-dimethylthiazol-2-yl]-2,5-diphenyl tetrazolium bromide (MTT, Sigma-Aldrich) assay, which measures the mitochondrial activity of viable cells [12]. At day 7 of culture, bone marrow-derived osteoblast cells were incubated with 10% MTT (5 mg/mL) in culture medium at 37 °C for 4 h. The medium was then aspirated from the well, and 1 mL acid isopropanol (0.04 N HCl in isopropanol) was added to each well. The plates were then stirred on a plate shaker for 5 min, and 150 μL of this solution was transferred to a 96-well format using opaque-walled transparent-bottomed plates (Corning). The optical density was read at 570–650 nm on the plate reader (μQuanti, BioTek Instruments Inc., Winooski, VT), and data were expressed as absorbance.

2.3.4. Extracellular matrix mineralization

At days 17 and 21 of bone marrow-derived osteoblast and preosteoblast MC3T3-E1 cell cultures, respectively, cells were fixed in 10% formalin for 2 h at RT, dehydrated and stained with 2% Alizarin Red S (Sigma-Aldrich), pH 4.2, for 10 min. The images were acquired using a high-resolution camera (Canon EOS Digital Rebel, 6.3 MP) and processed using Adobe Photoshop CS5.1 software (Adobe Systems). The calcium content was detected using a colorimetric method [13]. Briefly, 280 μL of 10% acetic acid were added to each well, and the plate was incubated at RT for 30 min under shaking. This solution was heated to 85 °C for 10 min, and transferred to ice for 5 min. The slurry was centrifuged at 20,000 g for 15 min, and 100 μL of the supernatant was mixed with 40 μL of 10% ammonium hydroxide. This solution was

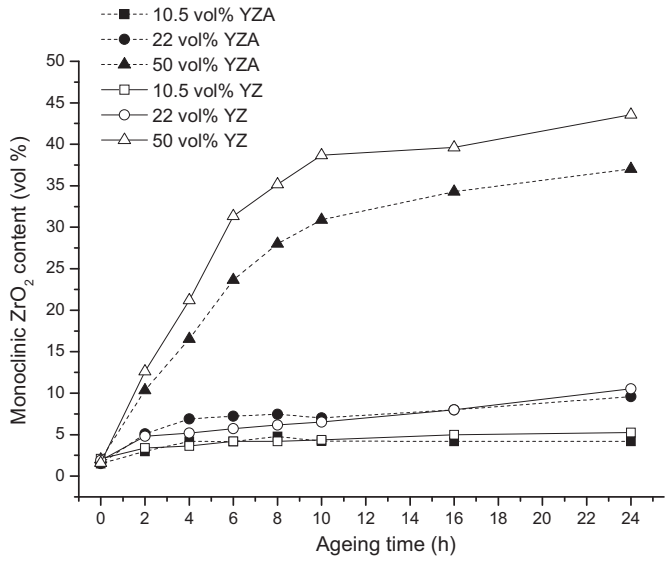

Fig. 1. Monoclinic zirconia content as a function of the ageing time for the different composites.

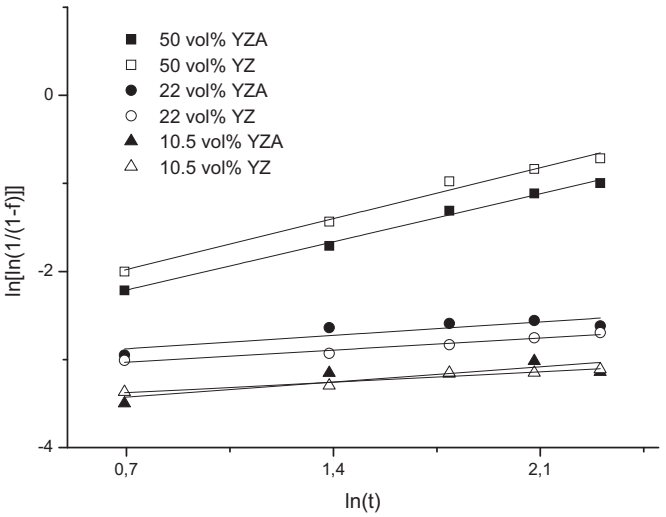

Fig. 2. ln[ln(1/1 − *f*)] versus ln (t) plots of the different Al_2O_3–ZrO_2 composites, using experimental data of Fig. 1.

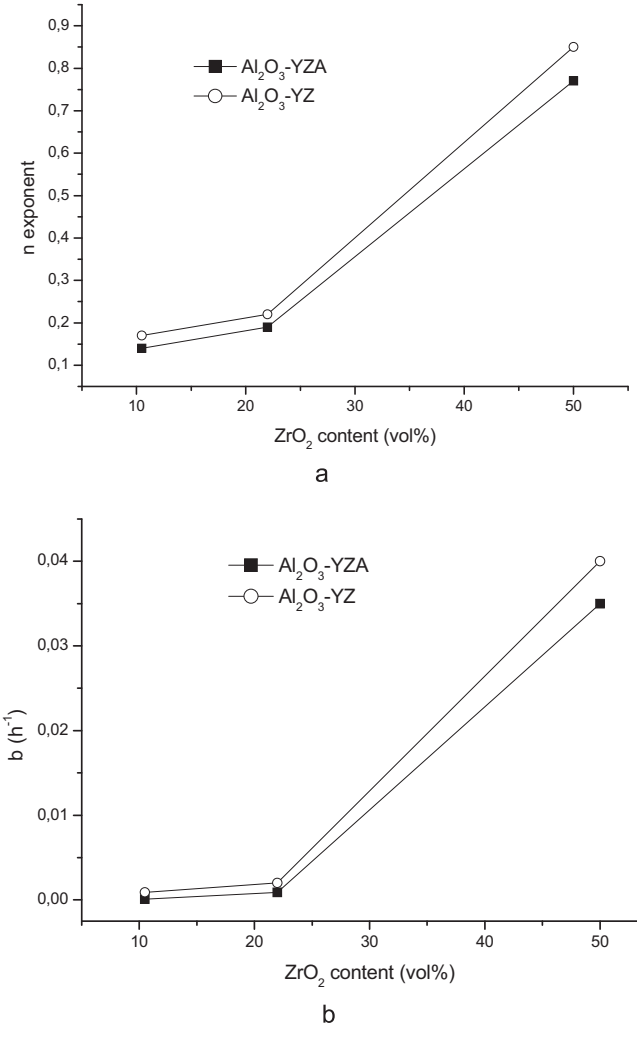

Fig. 3. *n* (a) and *b* (b) parameters of the MAJ equation as a function of the zirconia content for the different composites.

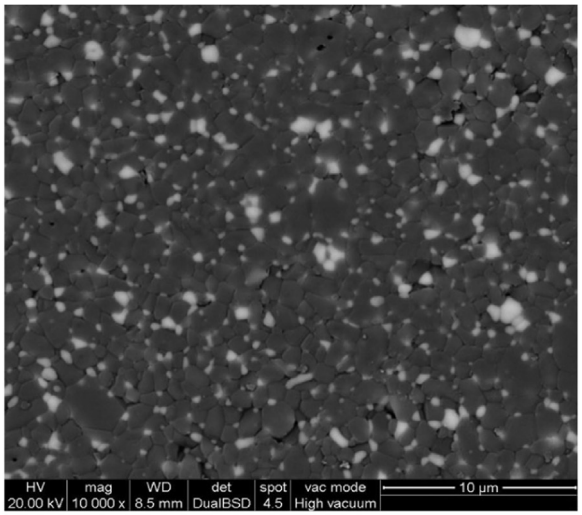

a

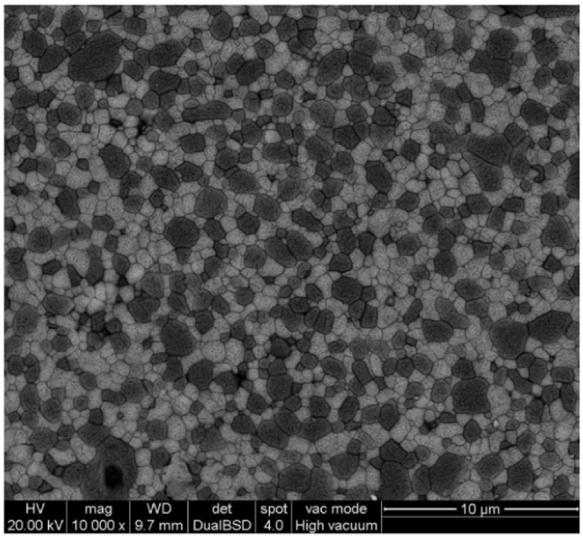

b

Fig. 4. SEM micrographs of Al_2O_3–ZrO_2 composites with different ZrO_2 contents: (a) 10.5 vol%, (b) 50 vol%. Bright grains (ZrO_2), dark grains (Al_2O_3).

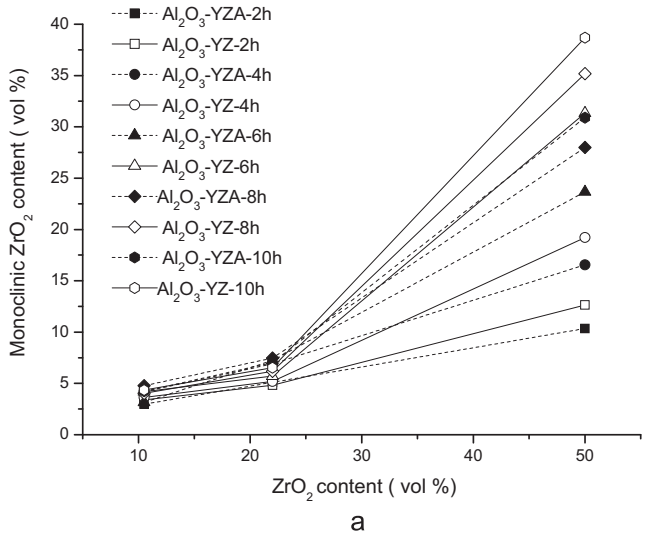

a

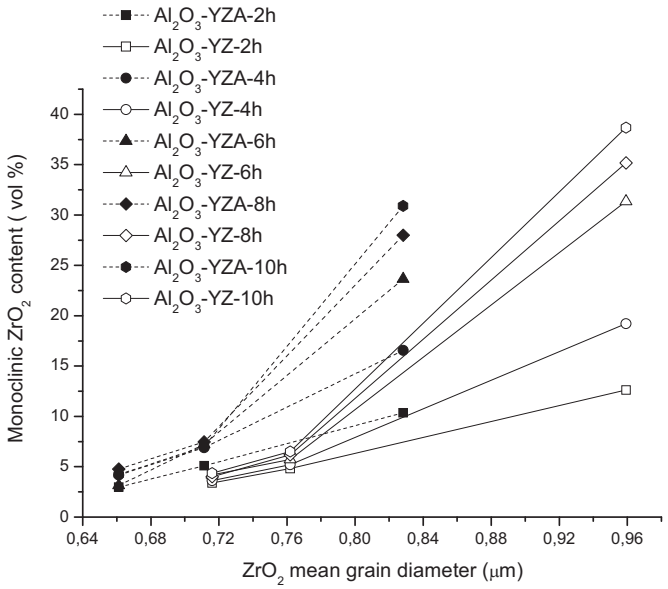

b

Fig. 5. Monoclinic ZrO_2 content as a function of the ZrO_2 content (a) and ZrO_2 mean grain diameter (b) in the different composites.

spectrophotometrically read at 405 nm in the plate reader µQuant (Biotek), and the data were expressed as absorbance.

2.3.5. Statistical analysis

The data were expressed as means ± standard deviations and analyzed by one-way ANOVA. Post-test was carried out by Tukey-b test when appropriate. For all comparisons, the level of significance (p) was set at 0.05.

3. Results and discussion

3.1. Ageing behavior

Low temperature degradation is thought to be the major detrimental influence on the long-term mechanical behavior of zirconia ceramics in the oral cavity. This degradation is due to a slow transformation from metastable tetragonal to the monoclinic phase, facilitated by the humid atmosphere [14]. There are several models that attempt to explain how the presence of water could promote tetragonal to monoclinic transformation in zirconia. Experimental results show that water radicals penetrate inside the zirconia lattice by dissolving Zr–O–Zr bonds [15]. Most probably, the oxygen of environmental water is located on vacancy sites and the hydrogen is placed on adjacent interstitial sites [13]. In Y-TZP, the presence of numerous vacancies due to the trivalent character of yttrium promotes the diffusion of water and thereby accelerates degradation [16]. The penetration of water radicals leads to a lattice contraction, which results in the formation of tensile stresses on the surface grains that destabilize the tetragonal phase; martensitic transformation of some grains at the surface can then take place. This nucleation of monoclinic phase leads to a cascade of events occurring neighbor to neighbor: the transformation of one grain leads to a volume increase stressing up the neighbor grains, and to micro-cracking. The micro-cracking offers a path for the water to penetrate down into the specimen.

It is generally accepted [3,17] that alumina–zirconia composites exhibited a less pronounced t-m transformation than Y-TZP. Since transformation of zirconia advances from grain to grain in a nucleation and growth process [17], the alumina matrix can retard progression of the transformation by reducing the contact area between zirconia grains.

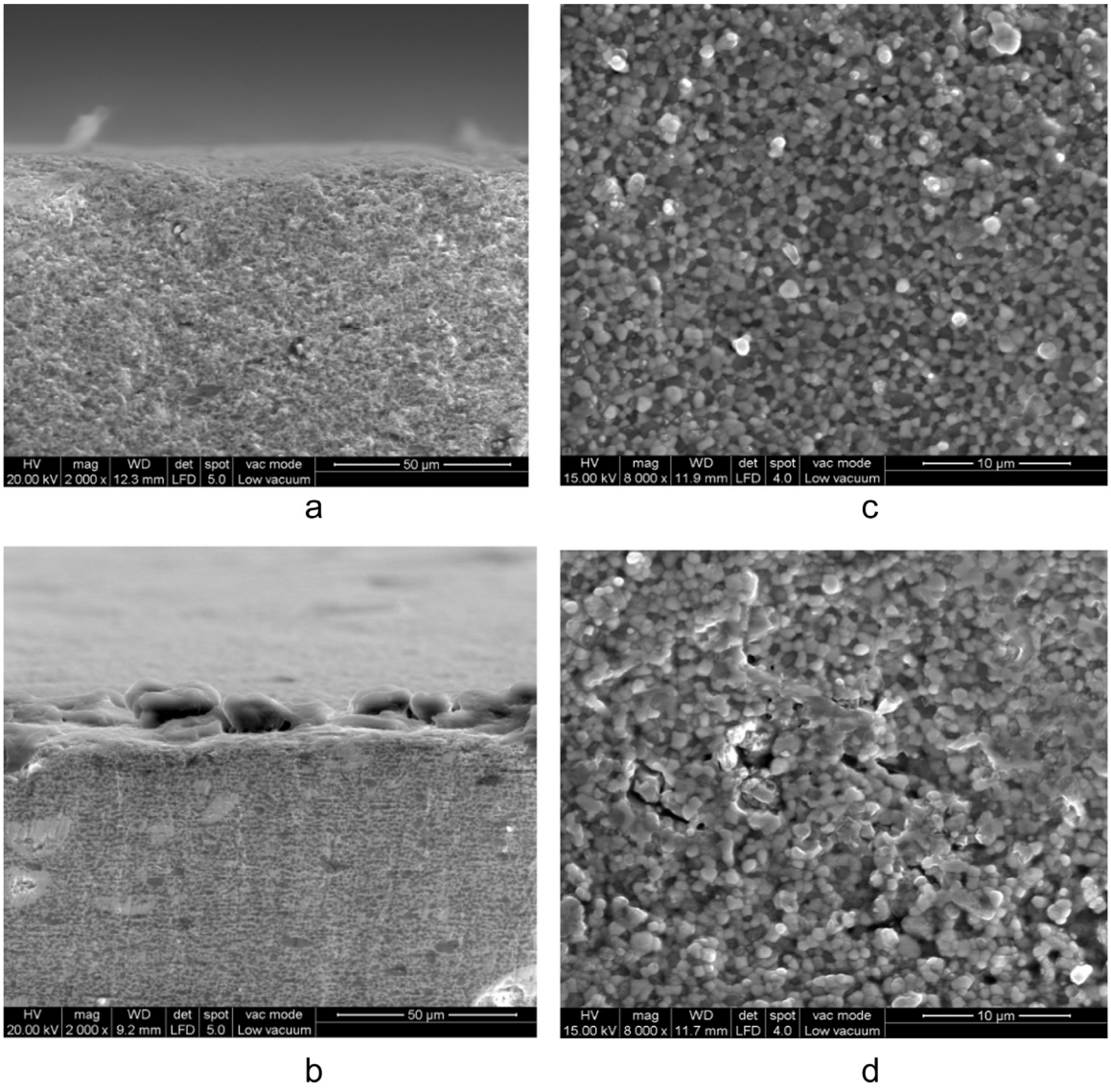

Fig. 6. SEM micrographs of the cross-section (a,b) and surfaces (c,d) of 50 vol% YZ: (a,c) before and (b,d) after 10 h of ageing.

The rate at which the tetragonal phase is transformed to monoclinic phase is an indication of the ageing sensitivity of the Al_2O_3–ZrO_2 ceramics [4]. Fig. 1 shows the monoclinic zirconia content as a function of the ageing time for the different composites. The monoclinic ZrO_2 content of the composites with 10.5 and 22 vol% ZrO_2 hardly changed with prolonged ageing time up to 24 h and remained below 8–9 vol% and 4–5 vol% for 22 and 10.5 vol% ZrO_2, respectively. The ageing susceptibility of Al_2O_3–ZrO_2 composites significantly increased with increasing the ZrO_2 content from 22 to 50 vol%. The curves of the composites with 50 vol% ZrO_2 quickly rose during the first 6 h of ageing, indicating that a nucleation process with constant rate occurred up to 6 h. For longer ageing time (>6 h) the lower slope observed was related with a reduction in the nucleation rate as the surface approached to its saturation level (i.e., when the surface is completely covered by the monoclinic nucleus) [18]; in this last period, a monoclinic content of 37 and 44 vol% was reached for 50 vol% YZA and 50 vol% YZ, respectively, after 24 h of ageing. For each ageing time, the amount of transformed monoclinic zirconia on the surface of 50 vol% YZ was greater than that of 50 vol% YZA.

Previous studies [7,19,20] have reported that the relationship between the amount of monoclinic phase and the aging time could be expressed by the Mehl–Arrami–Johnson (MAJ) equation which suggests nucleation and growth:

$$f = 1 - exp\left[-(b.\ t)^n\right] \quad (1)$$

where f is the transformation fraction, t is the time, b and n are constants dependent on the material. The n exponent which can be derived from the slope of the $\ln[\ln(1/1-f)]$ versus ln (t) plot, is related to nucleation and growth conditions; b is a thermally activated parameter that can be calculated from the ordinate origin of the $\ln[\ln(1/1-f)]$ versus ln (t) plot.

The $\ln[\ln(1/1-f)]$ versus ln (t) plots of the different Al_2O_3–ZrO_2 composites are shown in Fig. 2. Fig. 3a and b show the n and b parameters of the MAJ equation, respectively, as a function of the zirconia content for the different composites. A linear relationship between $\ln[\ln(1/1-f)]$ and ln (t) was observed for all the composites with a constant value of n lower than 1 (Figs. 2 and 3a). A value of n between 3 and 4 was observed for unconstrained zirconia (Y-TZP), where no matrix prevented the transformation. According to the MAJ theory, an n value between 3 and 4 corresponds to a nucleation and three-dimensional growth process. In the present study, for all the compositions n was kept below 1; according to Gremillard et al. [21], this n value suggested a mechanism in which nucleation predominated and growth proceeded at a lower rate.

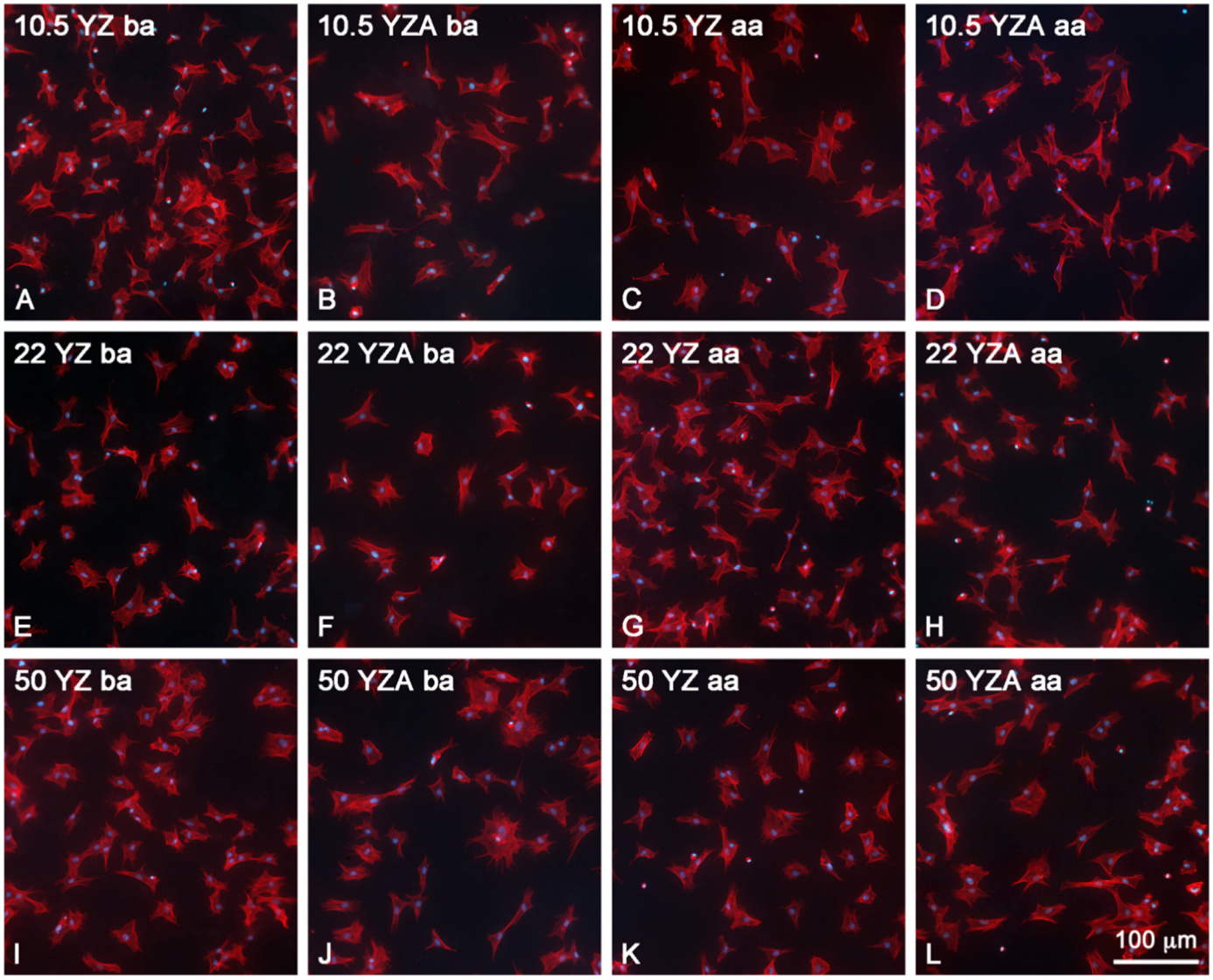

Fig. 7. Epifluorescence of bone marrow-derived osteoblast cell cultures grown on Al_2O_3-YZ (A, C, E, G, I, K) and Al_2O_3-YZA (B, D, F, H, J, L) disks with different ZrO_2 contents before ageing (ba) and after 2 h of ageing (aa) at day 1 of culture. Red and blue fluorescence indicate actin cytoskeleton and cell nuclei, respectively. Scale bar = 100 μm.

For the composites produced with YZ and YZA, a slightly increase in the n and b values and consequently in the t-m transformation rate with increasing the ZrO_2 content from 10.5 to 22 vol% was found, followed by a significant increase with further increasing the ZrO_2 content from 22 to 50 vol%. We have previously measured the variation of the Young's modulus (E) with the ZrO_2 content for the different composites; a nearly linear decrease of E with increasing the ZrO_2 content was found [2]. The addition of the lower elastic modulus ZrO_2 to Al_2O_3 decreased the elastic modulus of the composites. As the ZrO_2 content in the composites increased the constraint of the ZrO_2 grains was reduced (low E values) allowing the transformation to proceed. However, the n and b values (i.e., the transformation rate) were not found to vary linearly, as E, with the ZrO_2 content. This indicated that the transformation rate should be interpreted considering not only the restricting influence of the Al_2O_3 matrix on the transformation but also the microstructure of the composites.

For low ZrO_2 contents ($\leq$22 vol%), the majority of the ZrO_2 grains were isolated in the matrix (Fig. 4a), the Al_2O_3 matrix retarded progression of the transformation by reducing the contact area between zirconia grains. Thus, propagation of the transformation from one ZrO_2 grain to another was not possible. An increase in the ZrO_2 content over 22 vol% increased the contacts between ZrO_2 grains (Fig. 4b) approaching each other and promoting the propagation of the transformation. The transformation of a ZrO_2 grain triggered the transformation of a neighbor ZrO_2 grain; consequently the increase in the number of neighboring ZrO_2 grains in 50 vol% ZrO_2 allowed the transmission of the transformation shear strain. The existence of a zirconia percolation threshold of 16 vol% above which the transformation is propagating has been recently demonstrated [17]; in this work, a ZrO_2 percolation threshold of about 22 vol% was found. In the composites with 50 vol% ZrO_2, the reduced matrix elastic modulus enhanced the nucleation of monoclinic phase, and the increase in the ZrO_2 grains contacts allowed the propagation of the transformation.

Fig. 5a and b show the m-ZrO_2 content after 2–10 h of ageing as a function of the ZrO_2 concentration and the ZrO_2 mean grain diameter in the different composites, respectively. The monoclinic phase content of the composites with 10.5 and 22 vol% ZrO_2 slightly changed with prolonged ageing time up to 10 h (Fig. 5a). Although the average grain size of 10.5 vol% YZA (0.65 μm) and 22 vol% YZA (0.70 μm) were lower than those of 10.5 vol% YZ (0.72 μm) and 22 vol% YZ (0.77 μm), there was no marked

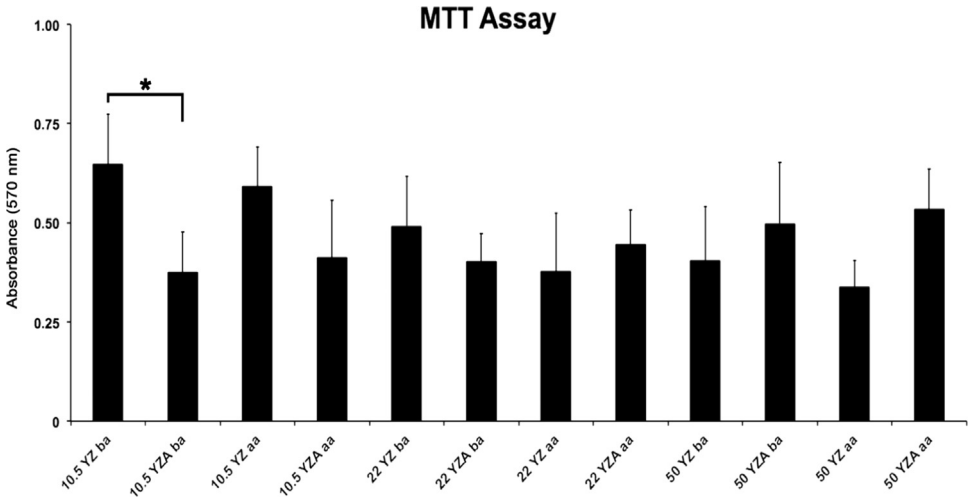

Fig. 8. MTT assay of bone marrow-derived osteoblast cell cultures grown on Al_2O_3-YZ and Al_2O_3-YZA disks with different ZrO_2 contents before ageing (ba) and after 2 h of ageing (aa) at day 7 of culture. The asterisk indicates statistically significant difference ($p < 0.05$).

difference in ageing behavior between these composites (Fig. 5b). In this particular case (ZrO_2 content ≤ 22 vol%), the grain size did not influence the transformability of t-ZrO_2 under ageing conditions.

The ageing susceptibility of the composites significantly increased with increasing the ZrO_2 content over 22 vol% (Fig. 5a), which could be attributed to the decrease in the matrix elastic modulus and the coalescence of the ZrO_2 grains. We have previously demonstrated [10] that the t-m phase transformation of YZ was similar to that of YZA, thus the transformation was not improved by Al_2O_3 doping. The tetragonal phase became easier to transform with increasing their size from 0.83 μm for 50 vol% YZA to 0.96 μm for 50 vol% YZ (Fig. 5b). In this work, there was a clear indication that the ZrO_2 grain size was the main factor affecting

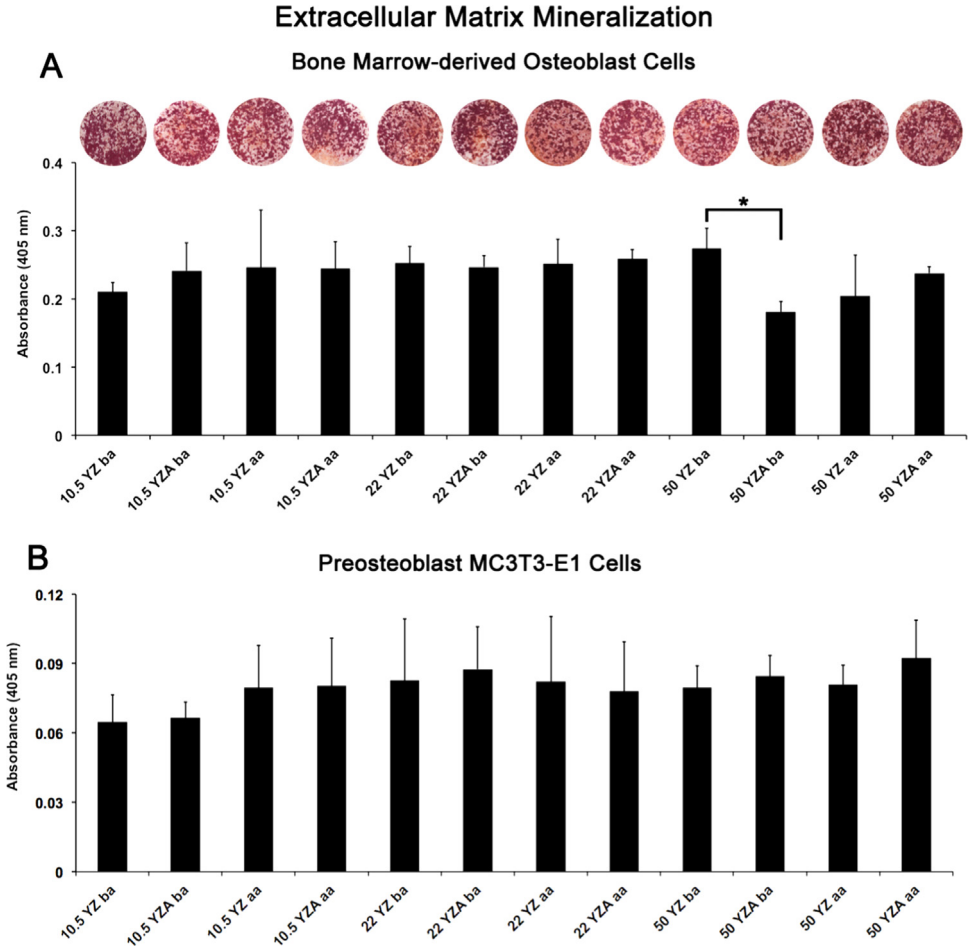

Fig. 9. Extracellular matrix mineralization (Ca content) of bone marrow-derived osteoblast (A) and preosteoblast MC3T3-E1 (B) cell cultures grown on Al_2O_3-YZ and Al_2O_3-YZA disks with different ZrO_2 contents before ageing (ba) and after 2 h of ageing (aa), at days 17 and 21 of culture, respectively. The asterisk indicates statistically significant difference ($p < 0.05$).

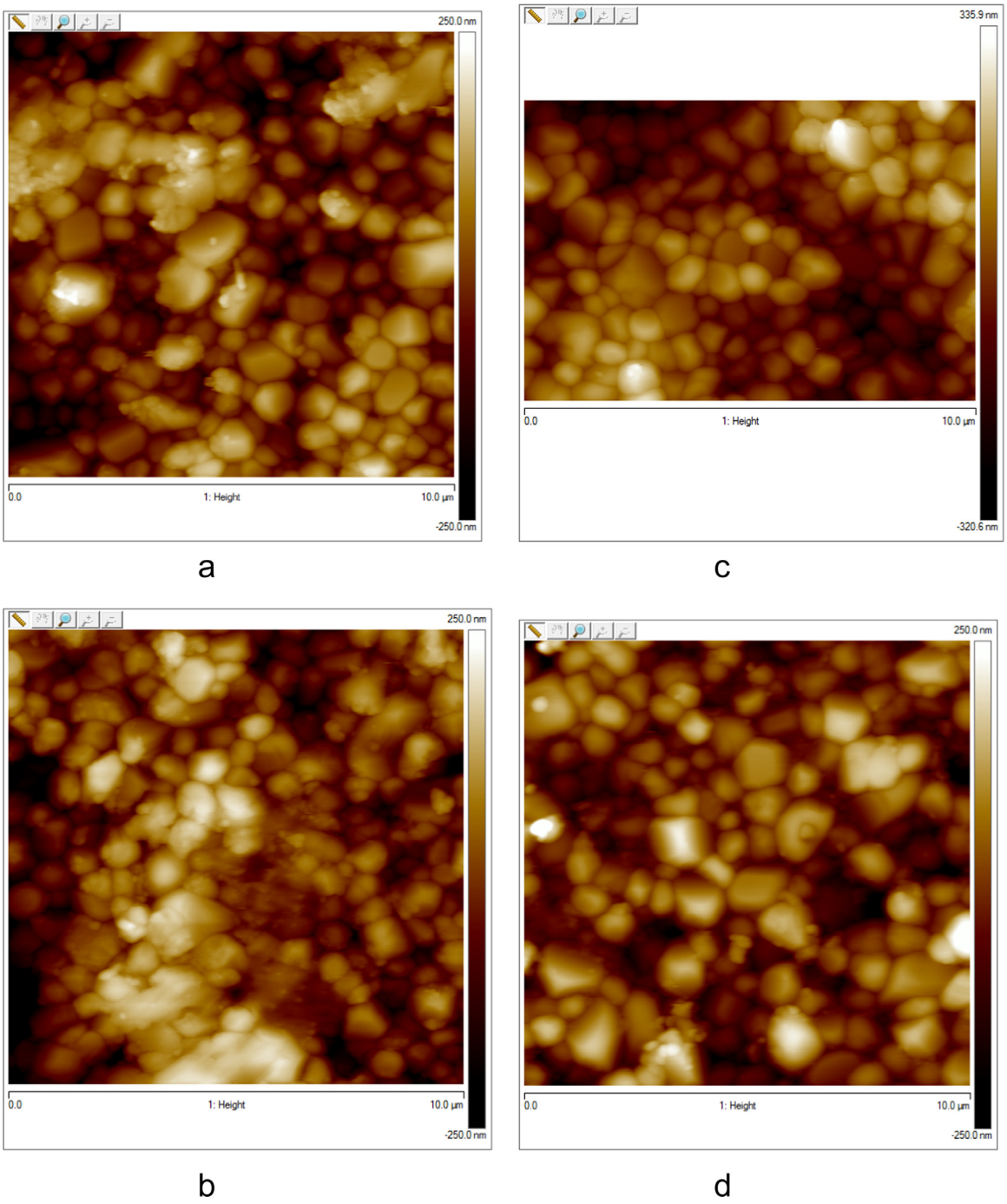

Fig. 10. AFM images of 50 vol% YZ (a, b) and 50 vol% YZA (c, d): before (a, c) and after (b, d) 2 h of ageing.

the transformability of t-ZrO_2 in the composites with 50 vol% ZrO_2. For each ageing time, the greater grain size of 50 vol% YZ with respect to 50 vol% YZA enhanced the ageing degradation.

Fig. 6a–d show SEM micrographs of the cross-section (a,b) and surfaces (c,d) of 50 vol% YZ before and after 10 h of ageing. Porosity, roughness and grain pullouts were visible on the specimen's surface after ageing (Fig. 6a–d). Surface uplift, roughness, microcracks and eventually grain pullout were produced on the sample's surface as a result of the volume expansion (4 vol%) associated with the t-m transformation.

3.2. Biological studies

The bone marrow-derived osteoblast cell response to the different composites was assessed in terms of cell morphology, viability and extracellular matrix mineralization at key time points, on days 1, 7 and 21 of culture, respectively. Fig. 7 shows the epifluorescence of bone marrow-derived osteoblast cell cultures grown on Al_2O_3-YZ and Al_2O_3-YZA discs at day 1 of culture. No major differences in terms of cell morphology were detectable among the composites. Overall, the cells adhered to and spread on the various substrates, exhibiting polygonal shapes and establishing cell-cell contact in some regions (Fig. 7). At day 7 of culture, despite some variations in the MTT values, there was statistical significant difference only for the comparison 10.5 vol% YZA ba and 10.5 vol% YZ ba (Fig. 8).

Fig. 9 shows the extracellular matrix mineralization (Ca

content) of bone marrow-derived osteoblast (Fig. 9a) and pre-osteoblast MC3T3-E1 (Fig. 9b) cell cultures grown on the different composites at days 17 and 21 of culture, respectively. Overall, there were no significant differences among groups in terms of osteogenic differentiation for both osteoblast cell culture models, except for the higher mineralization of bone marrow-derived osteoblast cells grown on 50 vol% YZ ba compared with the ones grown on 50 vol% YZA ba. The presence of higher amounts of Zr-OH functional groups on the YZ surface with respect to YZA could positively affect osteoblast cell functions, as demonstrated elsewhere [22]. Besides, the isoelectric point (IEP) of YZA (pH_{IEP}=8.9, Table 1) was higher than that of Al_2O_3 (pH_{IEP}=8 [2]) and YZ (pH_{IEP}=7, Table 1), therefore the substitution of either 50 vol% Al_2O_3 or 50 vol% YZ by 50 vol% YZA resulted in a markedly decreased in the negative surface charge of 50 vol% YZA surface in the culture medium. Both the decrease in the negative surface charge and the lesser amount of Zr-OH functional groups on 50 vol% YZA ba reduced the osteogenic potential of the bone marrow-derived osteoblast cell cultures. Despite that, no similar effect was observed when the preosteoblast MC3T3-E1 cells were evaluated. In *in vitro* experiments of biomaterials for bone applications, one can expect differences between primary cells and cell lines in terms of key parameters of the acquisition of the osteogenic phenotype, a finding that has been described and discussed elsewhere [23].

For Al_2O_3-YZA composites before ageing, a tendency toward a decrease in the mineralization of bone marrow-derived osteoblast cells was found with increasing the YZA content from 22 to 50 vol%, which was probably due to the decrease in the negative surface charge of 50 vol% YZA surface in the culture medium.

2 h of ageing was chosen to study the effect of ageing on the osteogenic differentiation of the various Al_2O_3–ZrO_2 surfaces. There were no significant differences in the osteogenic differentiation after ageing on the composites with 10.5 and 22 vol% ZrO_2. The ageing process tended to rescue the osteogenic potential of bone marrow-derived osteoblast cells grown on 50 vol% YZA while inhibiting the one on 50 vol% YZ. The higher t-m transformation on 50 vol% YZ compared to 50 vol% YZA (Figs. 1 and 2) appeared to be not favorable for the osteogenic differentiation.

The AFM images of 50 vol% YZ and 50 vol% YZA obtained before and after the ageing process are represented in Fig. 10a–d. On the ZrO_2 grains presenting a phase transformation from tetragonal to monoclinic, it could be observed an increase in the brightness of the grains. The increase in brightness was directly due to a height increase of ZrO_2 grains after the ageing process. The AFM images after ageing clearly revealed a greater difference in brightness in 50 vol% YZ compared with 50 vol% YZA. This behavior was attributed to the greater number of t-ZrO_2 grains transformed to m-ZrO_2 in 50 vol% YZ after ageing. The modified relief of the ZrO_2 grains, which had undergone the t-m transformation, led to surface roughness; thus, the sample's surface became rougher after ageing. The average roughness, calculated from AFM analysis, of 50 vol% YZA increased from 70 to 88.3 after 2 h of ageing, whereas that of 50 vol% YZ increased from 68.3 to 98.4. For 50 vol% YZ, a larger increase in surface roughness was observed, in accordance with the more pronounced t-m transformation (Figs. 1 and 2). It is generally accepted that the material surface roughness at the micron and nanoscale enhances bone matrix production at the material/tissue interface *in vitro* and *in vivo* [24]. The lesser surface roughness of 50 vol% YZA aa compared with 50 vol% YZ aa was found to be favorable for the progression and extracellular matrix mineralization of the bone marrow-derived osteoblast cell cultures; on the contrary, the high level of roughness of 50 vol% YZ aa appeared to be not favorable (Fig. 9a). There seemed to be a narrow surface roughness range between improvement and reduction of the osteogenic potential of bone marrow-derived osteoblast cells.

4. Conclusions

The influence of the ZrO_2 content and ZrO_2 grain size on the ageing behavior of two different Al_2O_3–ZrO_2 composites was studied. In addition, the biocompatibility and osteogenic differentiation of the different Al_2O_3–ZrO_2 surfaces were evaluated before and after ageing using osteoblast cell cultures. When the volume fraction of ZrO_2 was kept under 22 vol%, the ageing susceptibility was reduced independently from the ZrO_2 grain size. The ZrO_2 ageing degradation significantly increased with increasing the ZrO_2 content from 22 to 50 vol%; the greater grain size of 50 vol% YZ with respect to 50 vol% YZA enhanced the ageing degradation.

Overall, no significant differences among the composites before ageing were observed in terms of osteogenic differentiation, except for the higher mineralization of bone marrow-derived osteoblast cells grown on 50 vol% YZ ba compared with 50 vol% YZA ba. The ageing process tended to rescue the osteogenic potential of these cells grown on 50 vol% YZA while inhibiting the one on 50 vol% YZ. In conclusion, the low ageing sensitive of the composites with ZrO_2 contents $\leq$22 vol% did not change the osteoblast biocompatibility, whereas the greater ageing degradation of the composites with 50 vol% ZrO_2 seemed to alter the osteogenic potential of bone marrow-derived osteoblast cells.

Acknowledgments

This work was financially supported by CONICET (2012/Res. D. No ° 2544) and FAPESP 2012/50949-4.

References

[1] S. Olhero, I. Ganesh, P. Torres, F. Alves, J.M.F. Ferreira, Aqueous colloidal processing of ZTA composites, J. Am. Ceram. Soc. 92 (2009) 9–16.
[2] H.L. Calambás Pulgarin, M.P. Albano, Three different alumina–zirconia composites: Sintering, microstructure and mechanical properties, Mat. Sci. Eng. A 639 (2015) 136–144.
[3] S. Deville, J. Chevalier, C. Dauvergne, G. Fantozzi, J. Bartolomé, J.S. Moya, R. Torrecillas, Microstructural investigation of the aging behavior of (3Y-TZP)–Al_2O_3 composites, J. Am. Ceram. Soc. 88 (2005) 1273–1280.
[4] T. Kosmac, A. Koljan, Ageing of dental zirconia ceramics, J. Eur. Ceram. Soc. 32 (2012) 2613–2622.
[5] A.H. de Aza, J. Chevalier, G. Fantozzi, M. Schehl, R. Torrecillas, Slow-crack-growth behavior of zirconia-toughened alumina ceramics processed by different methods, J. Am. Ceram. Soc. 86 (2003) 115–120.
[6] L. Hallmann, P. Ulmer, E. Reusser, M. Louvel, C.H.F. Hammerle, Effect of dopants and sintering temperature on microstructure and low temperature degradation of dental Y-TZP-zirconia, J. Eur. Ceram. Soc. 32 (2012) 4091–4104.
[7] J. Chevalier, S. Deville, E. Munch, R. Jullian, F. Lair, Critical effect of cubic phase on aging in 3 mol% yttria-stabilized zirconia ceramics for hip replacement prosthesis, Biomaterials 25 (2004) 5539–5545.
[8] D. Balzar, N.C. Popa, Analyzing microstructure by Rietveld refinement, Rigaku J. 22 (2005) 16–25.
[9] C. Maniatopoulos, J. Sodek, A.H. Melcher, Bone formation *in vitro* by stromal cells obtained from bone marrow of young adult rats, Cell. Tissue Res. 254 (1988) 317–330.
[10] Y.L. Bruni, L.B. Garrido, M.P. Albano, L.N. Teixeira, A.L. Rosa, P.T. de Oliveira, Effects of surface treatments on Y-TZP phase stability, microstructure and osteoblast cell response, Ceram. Int. 41 (2015) 14212–14222.
[11] H.O. Schwartz, Fo, A.B. Novaes Jr., L.M.S. de Castro, A.L. Rosa, P.T. de Oliveira, *In vitro* osteogenesis on a microstructured titanium surface with additional submicron-scale topography, Clin. Oral. Implant. Res. 18 (2007) 333–344.
[12] T. Mosmann, Rapid colorimetric assay for cellular growth and survival: application to proliferation and cytotoxicity assays, J. Immunol. Methods 65 (1983) 55–63.
[13] C.A. Gregory, W.G. Gunn, A. Peister, D.J. Prockop, An Alizarin red-based assay of mineralization by adherent cells in culture: comparison with cetylpyridinium chloride extraction, Anal. Biochem. 329 (2004) 77–84.
[14] F. Zhang, K. Vanmeensel, M. Inokoshi, M. Batuk, J. Hadermann, B. Van Meerbeek, I. Naert, J. Vleugels, 3Y-TZP ceramics with improved hydrothermal degradation resistance and fracture toughness, J. Eur. Ceram. Soc. 34 (2014) 2453–2463.
[15] T. Sato, M. Shimada, Transformation of yttria-doped zirconia polycrystals by annealing in water, J. Am. Ceram. Soc. 68 (1985) 356–359.
[16] Y.S. Kim, C.H. Jung, J.Y. Park, Low temperature degradation of yttria-stabilized tetragonal zirconia polycrystals under aqueous solutions, J. Nucl. Mater. 209

(2012) 326–331.
[17] P. Kohorst, L. Borchers, J. Strempel, M. Stiesch, T. Hassel, F.W. Bach, C. Hubsch, Low-temperature degradation of different zirconia ceramics for dental applications, Acta Biomater. 8 (2012) 1213–1220.
[18] C. Pecharroman, J.F. Bartolome, J. Requena, J.S. Moya, S. Deville, J. Chevalier, G. Fantozzi, R. Torrecillas, Percolative mechanism of aging in zirconia-containing ceramics for medical applications, Adv. Mater. 15 (2003) 507–511.
[19] J.R. Kelly, I. Denry, Stabilized zirconia as a structural ceramic: an overview, Dent. Mater. 24 (2008) 289–298.
[20] K. Matsui, H. Horikoshi, N. Ohmichi, M. Ohgai, H. Yoshida, Y. Ikuhara, Cubic-formation and grain-growth mechanisms in tetragonal zirconia polycrystal, J. Am. Ceram. Soc. 86 (2003) 1401–1408.
[21] L. Gremillard, J. Chevalier, T. Epicier, S. Deville, G. Fantozzi, Modeling the aging kinetics of zirconia ceramics, J. Eur. Ceram. Soc. 24 (2004) 3483–3489.
[22] S. Zhang, J. Sun, Y. Xu, S. Qian, B. Wang, F. Liu, X. Liu, Adhesion, proliferation and differentiation of osteoblasts on zirconia films prepared by cathodic arc deposition, Biomed. Mater. Eng. 23 (2013) 373–385.
[23] E.M. Czekanska, M.J. Stoddart, R.G. Richards, J.S. Hayes, In search of an osteoblast cell model for *in vitro* research, Eur. Cell. Mater. 24 (2012) 1–17.
[24] R.A. Gittens, R. Olivares-Navarrete, A. Cheng, D.M. Anderson, T. McLachlan, I. Stephan, J. Geis-Gerstorfer, K.H. Sandhsge, A.G. Fedorov, F. Rupp, B.D. Boyan, R. Tannenbaum, Z. Schwartz, The roles of titanium surface micro/nanotopography and wettability on the differential response of human osteoblast lineage cells, Acta Biomater. 9 (2013) 6268–6277.